Available online at www.sciencedirect.com
ScienceDirect
Ceramics International 37 (2011) 293–301
CERAMICS INTERNATIONAL
www.elsevier.com/locate/ceramint

Processing and properties of ZrB_2–SiC composites obtained by aqueous tape casting and hot pressing

Zhihui Lü [a,b], Dongliang Jiang [a,*], Jingxian Zhang [a], Qingling Lin [a]

[a] State Key Laboratory of High Performance Ceramics and Superfine Microstructures, Shanghai Institute of Ceramics, Chinese Academy of Sciences, Shanghai 200050, PR China
[b] Graduate University of the Chinese Academy of Sciences, Beijing 100049, PR China

Received 16 April 2010; received in revised form 21 July 2010; accepted 28 August 2010
Available online 29 September 2010

Abstract

ZrB_2–SiC composites with different SiC content were prepared through aqueous tape casting and hot pressing. The influences of dispersant, SiC content and binder content on the rheological properties of slurries were investigated and the conditions for preparing stable ZrB_2–SiC suspensions were optimized. After tape casting and drying, the green ZrB_2–SiC tapes showed good flexibility, lubricious surface and homogeneous microstructure. The ZrB_2 ceramics could be densified to 97.2% after hot-pressing, while the ZrB_2 containing 20 and 30 vol% SiC ceramics were nearly fully densified (>99%). The sintered ZrB_2–20 vol% SiC ceramic had improved mechanical properties compared with ZrB_2 ceramic. Further increase in SiC content resulted in lower flexural strength and fracture toughness. SEM and TEM showed a fine microstructure with a clear grain boundary. The fracture mode changed from intragranular type for ZrB_2 to both intragranular and intergranular type for ZrB_2–SiC composites.

Keywords: A. Suspensions; A. Tape casting; C. Mechanical properties; ZrB_2–SiC; Microstructure

1. Introduction

The interest in ultra-high temperature ceramics (UHTCs) has increased significantly in recent years [1–3] due to their remarkable properties, such as high melting point, high thermal conductivities, excellent corrosion resistance and good oxidation resistance [4–6], which make them promising candidates for high-temperature structural applications. Among the UHTCs, ZrB_2 is of particular interest due to its lower theoretical density (6.09 g/cm^3) and lower cost, which can be an advantage over other candidates for aerospace applications [5]. Several studies have demonstrated that the addition of SiC could improve the oxidation resistance and mechanical properties of ZrB_2 ceramics [7–13], so a lot of works have been carried out on ZrB_2–SiC ceramics.

Nowadays, colloidal processing [14], which can produce a more homogeneous green microstructure [15–17], is becoming more and more important in the fabrication of advanced ceramics because it offers the potential to produce reliable ceramic films and bulk forms through careful control of initial suspension ''structure'' and its evolution during fabrication [18]. Among the colloidal processing methods, tape casting is a widespread and cost-effective one mainly used to make thin and flat ceramic sheets [19–21]. Moreover, it can be used to build up multilayered structures with complex geometries and improved properties, such as higher fracture toughness [22] and better thermal shock behavior [23]. In our previous research, aqueous tape casting of zirconium diboride has been well studied [24]. However, up to now, there is rarely report on the co-dispersion and tape casting of ZrB_2 and SiC.

In the present work, the co-dispersion of ZrB_2 and SiC slurries was studied in terms of zeta potential and rheological tests. Well de-agglomerated ZrB_2/SiC slurries suitable for tape casting were obtained, and ZrB_2/SiC green sheets with

* Corresponding author. Tel.: +86 21 5241 2606; fax: +86 21 5241 3122.
E-mail address: dljiang@sunm.shcnc.ac.cn (D. Jiang).

0272-8842/$36.00
doi:10.1016/j.ceramint.2010.08.044

high quality were prepared. The properties of as-sintered ZrB_2/SiC composites were also investigated.

2. Experimental procedure

2.1. Starting materials and processing

Commercially available ZrB_2 powders (average particle size ~3.2 μm, oxygen content 3.0 wt%, Dandong Chemical Engineering Institute Co. Ltd., China), B_4C powders (average particle size as 0.93 μm and a specific surface area as 10.78 m^2/g) and SiC powders (0.6 μm, α-phase, FCP 15C, Sika Tech., Norway) were used as raw materials. Lopon 885, an ammonium polyacrylate solution (39–41% PAA-NH_4, BK Giulini, Germany, M_w = 4000–5000, pH 7–8) was used as the dispersant. A commercial aqueous polymer emulsion (Nacrylic 4700, glass transition temperature $T_g = -22\,^{\circ}C$, National Starch & Chemical, USA), with solid content of 50 wt% and particle size of 0.10–0.30 μm, was used as the binder. A commercial ester alcohol (Texanol, Eastman, USA) was used as the plasticizer to improve the film integrity. ZrB_2–SiC suspensions were designated by the letters ZS (for ZrB_2 and SiC) along with the SiC content (based on total ceramic powder). For example, the suspension prepared from ZrB_2 and 20 vol% SiC was designated as ZS20.

The as-received ZrB_2 was attrition milled for 2 h at 300 rpm followed by acid treatment. The details of the processing have been reported previously [24]. Aqueous ZrB_2 slurries were prepared by mixing as-treated ZrB_2 powder, B_4C powder and dispersant into distilled water. Aqueous ZrB_2–SiC slurries were prepared by mixing as-treated ZrB_2 powder, SiC powder and dispersant into distilled water similarly. Slurries were ball milled with zirconia media for 24 h, followed by adding emulsion binder and plasticizer. Then the slurries were ball milled for another 12 h. After homogenization, the slurries were degassed under vacuum to remove air bubbles. Finally, tape casting was performed on Procast Precision Tape Casting Equipment (Division of the International, Inc., USA) with a gap height of 400 μm at a speed of 100 mm/min. The shear rate was calculated to be ~4 s^{-1}. After drying freely in open air at ambient temperature for 4–5 h, green tapes were obtained. The green tapes were laminated and heat treated at 500 °C for 1 h to remove the binder. Then, the pyrolysed tapes were sintered at 1900 °C and 2000 °C for 45 min under an applied pressure of 32 MPa in Ar atmosphere [25].

2.2. Characterization

ZrB_2 and SiC suspensions (0.01 vol%) in the absence and presence of dispersant were prepared, respectively, for zeta potential analysis using Zetaplus (Brookhaven Instruments Corp., USA). The Rheological behavior of ZrB_2–SiC suspensions were investigated using parallel-plate system on Universal Stress Rheometer SR5 (Rheometric Scientific Inc., USA). The tensile test of green tapes was performed at a constant load speed and a span length of 10 mm/min and 20 mm, respectively, using a computer-controlled INSTRON universal testing machine (Model 5566, Instron Corp., UK). The density of green tapes and as-sintered ceramics were measured using Archimedes method with alcohol and water as the immersing media, respectively. The microstructure of the sintered body was observed by scanning electron microscopy (JXA 8100, Jeol, Tokyo, Japan) and transmission electron microscopy (TEM: JEM2100F). The grain boundary was observed by high resolution transmission electron microscopy (HRTEM). Flexural strength was tested in three-point bending on 3.0 mm × 4.0 mm × 36.0 mm bars, using a span width of 30 mm and a crosshead speed of 0.5 mm/min (Model 5566, Instron Corp.). Elastic modulus was calculated by the bending method based on the Chinese Standard GB/T 10700-2006. Microhardness (Hv1.0) was measured by Vickers' indentation with a load of 9.8 N and a holding time of 10 s (Wilson-wolpert Tukon 2100B, Instron Corp.). Fracture toughness was measured by indentation test with a load of 49.8 N and a hold time of 10 s. The average grain size for different samples was calculated using the linear intercept method. At least 100 grains were measured to get the average value.

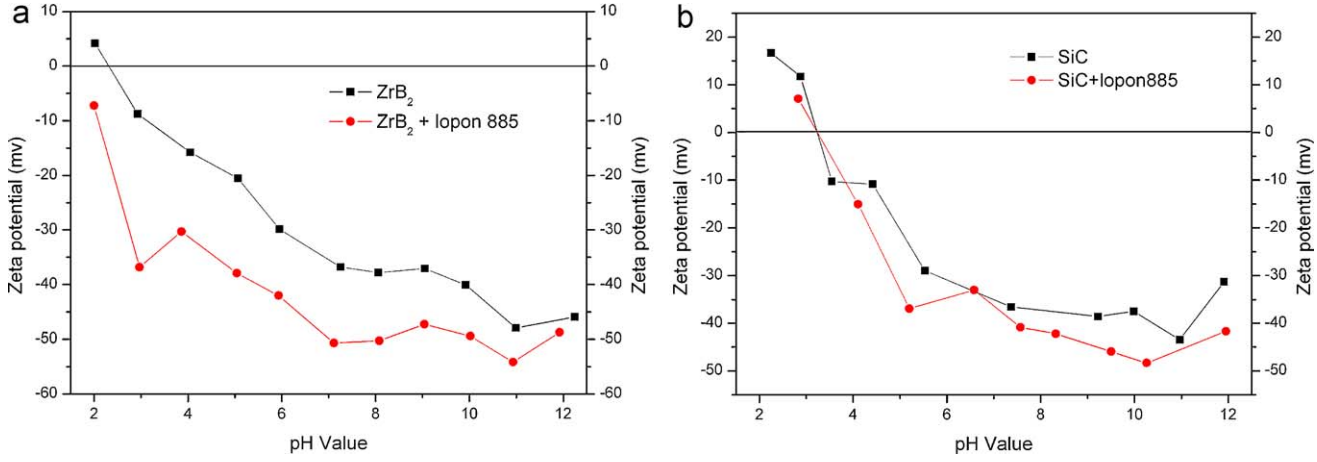

Fig. 1. Zeta potential of ZrB_2 and SiC with and without Lopon 885.

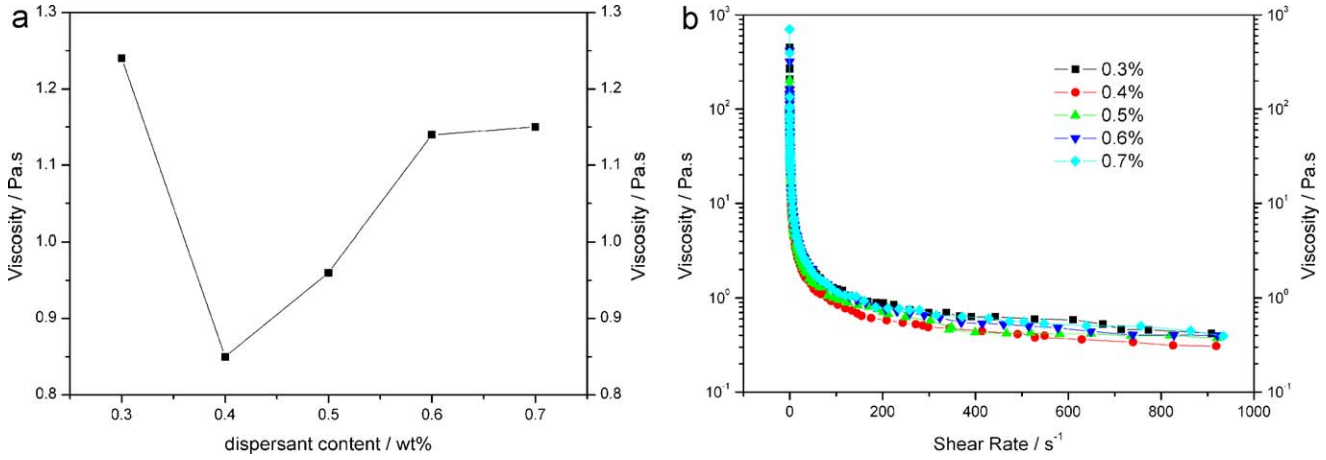

Fig. 2. Effect of dispersant content on (a) the viscosity at 100 s^{-1} and (b) rheological behavior of 40 vol% ZS20 suspensions (pH = 9).

3. Results and discussion

3.1. Surface properties of ZrB_2 and SiC

Electrostatic repulsion forces, which are generated by common surface charges among particles, offer the sources of stabilization of the suspensions. Another effect, steric hindrance can also help the stabilization [26]. The zeta potential is a commonly used parameter used to describe the surface charge behavior of the particles in the suspensions. Lopon 885 had been demonstrated to be effective for the aqueous dispersion of ZrB_2 in basic pH range because its addition led to an obvious increase of negative charge density on ZrB_2 particle surface (Fig. 1(a)) [24]. Although the negative charge density on SiC particle surface showed no obvious increase after adding Lopon 885 (Fig. 1(b)), the co-dispersion of ZrB_2 and SiC in the alkaline pH range could still be achieved due to their similar highly electronegative zeta potential values (∼−50 mV). Therefore, in this paper, the ZrB_2–SiC suspensions are also stabilized using Lopon 885 as the dispersant. As the surface charge density almost kept constant at basic pH region, the slurry pH was kept at around pH 9 without further screen, similar to that reported in the literature [24].

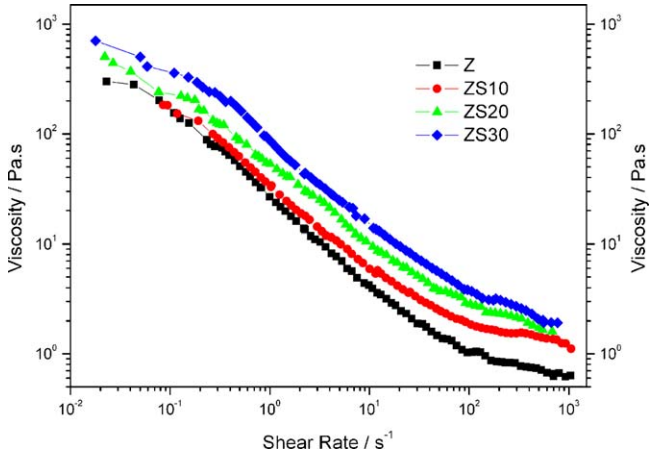

Fig. 3. Viscosity of 45 vol% ZS suspensions with different SiC content (pH = 9).

3.2. Effect of dispersant content

The effect of dispersant content (based on ceramic powder) on the viscosity of 40 vol% ZS20 suspensions was characterized in terms of viscosity and rheological measurements (Fig. 2). The viscosity of ZS20 suspensions decreased with the addition of Lopon 885 up to 0.4 wt% and increased thereafter (Fig. 2(a)). The same trend had been observed for 40 vol% ZrB_2 suspensions (without SiC) with the addition of Lopon 885 [24]. The addition of SiC showed no obvious influence on the optimum dispersant content. Therefore, 0.4 wt% of dispersant is appropriate for the co-dispersion of ZrB_2 and SiC powders in aqueous media. This conclusion was further confirmed by the rheological measurements (Fig. 2(b)).

3.3. Effect of SiC content

Based on the conclusion above, ZS suspensions containing different content of SiC (0–30 vol%) with a fixed total solid content of 45 vol% were successfully prepared at the selected pH and dispersant content (Fig. 3). The viscosity of ZS suspensions increased with the increase of SiC content. There may be two reasons for that: First, the dispersion effect of Lopon 885 for SiC was weaker than that for ZrB_2; Second, the different surface properties of ZrB_2 and SiC could also result in the formation of weak agglomerates and the increase of viscosity. However, all the slurries were in well stabilized state and exhibited shear thinning behavior.

3.4. Influence of binder content

Binders are added to suspensions in order to get flexible membranes with enough strength for easy handling and storage. The binder forms organic interparticle bridges in the tape, resulting in a strong cohesion after solvent evaporation. In our

Table 1
Suspension viscosity and properties of ZrB_2 green tapes.

Binder name	Binder content (wt%)	η (4 s^{-1}) (Pa s)	Tensile strength (MPa)	Green density (g cm^{-3})	Remarks
Nacrylic 4700	4	3.0	1.65 ± 0.18	3.04 ± 0.05	Cracks
	6	1.4	2.03 ± 0.07	3.11 ± 0.11	–
	8	1.2	2.12 ± 0.03	2.94 ± 0.02	–
	10	1.1	2.16 ± 0.11	2.92 ± 0.03	–
Mowilith DM 765 [24]	18	6.1	1.21 ± 0.06	2.82 ± 0.03	–

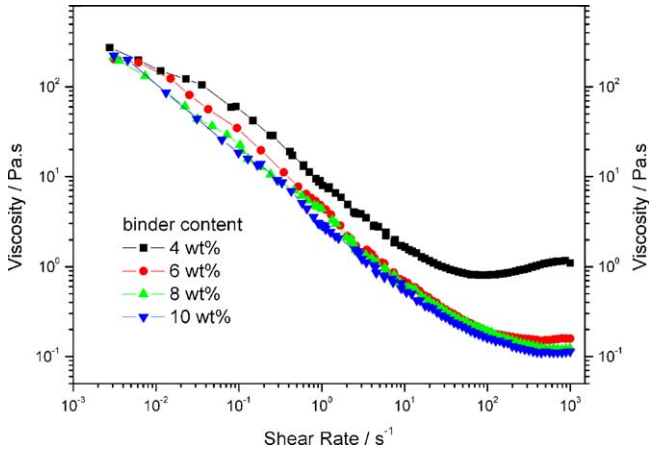

Fig. 4. Rheological properties of ZrB_2 suspensions with different binder content.

previous report, a commercial aqueous polymer emulsion, Mowilith DM 765, was selected as the binder for aqueous tape casting of ZrB_2 [24]. The minimum content of this binder to form crack-free ZrB_2 green tapes was determined to be 18 wt%. In tape casting, it is important to obtain high solid content slurry because the solid content of the suspension directly corresponds to the green density of the sheets. Furthermore, low amounts of water to be evaporated during drying and of organic additives to be burned out could reduce the risk of defect formation [27]. Hereby, another acrylic emulsion binder (Nacrylic 4700), which could effectively reduce the binder content, was used for aqueous tape casting of ZrB_2–SiC.

For ZrB_2 suspensions with 6 wt% B_4C as sintering additives, different amounts of binder were added to the suspensions and the influence of binder content was studied (Table 1 and Fig. 4). The suspension viscosity at 4 s^{-1} decreased from 3.0 to 1.1 Pa s when binder content (based on ceramic powder) increased from 4 wt% to 10 wt%. The green density decreased with the increase in binder content too. The exception was the tape with 4 wt% binder, which had a lower green density than the tape with 6 wt% binder. This could be attributed to its high slurry viscosity, which might prevent the rearrangement of the powder after passing the blade. The increase of binder content led to the increase of coalescent force and consequently resulted in the increase of tensile strength. The suspensions containing 6 wt%, 8 wt% and 10 wt% binder showed shear thinning behavior, which is suitable for tape casting. However, with the binder content decreased to 4 wt%, the suspension displayed shear thickening behavior at the shear rate of about 80 s^{-1}. Based on the discussion above, the optimum amount of binder content for ZrB_2 was found to be 6 wt%. The green density and tensile strength of green sheets after drying were 3.11 g cm^{-3} and 2.03 MPa, respectively.

For ZS20 suspensions, the influence of binder content was also studied (Table 2 and Fig. 5). Results were similar to those for ZrB_2 green tapes. Comparing with ZrB_2, SiC had a lower density, so the green densities of ZS20 green tapes were lower than that of ZrB_2 ones with the same binder content. In addition, the tensile strength of ZS20 green tapes was also lower than that of ZrB_2 ones, which indicated that the binder had lower cohesion for SiC than for

Table 2
Suspension viscosity and properties of ZS20 green tapes.

Powder composition	Binder content (wt%)	η (4 s^{-1}) (Pa s)	Tensile strength (MPa)	Green density (g cm^{-3})	Remarks
ZS20	6	5.0	1.30 ± 0.15	2.71 ± 0.01	Cracks
	8	3.5	1.54 ± 0.18	2.65 ± 0.03	–
	10	2.3	1.67 ± 0.03	2.61 ± 0.11	–

Table 3
Suspension viscosity and properties of ZS green tapes.

Powder composition	Binder content (wt%)	η (4 s^{-1}) (Pa s)	Tensile strength (MPa)	Green density (g cm^{-3})
Z	6	1.4	2.03 ± 0.07	3.11 ± 0.11
ZS10	6	2.7	1.72 ± 0.07	2.81 ± 0.02
ZS20	8	3.5	1.54 ± 0.07	2.65 ± 0.03
ZS30	10	5.4	1.42 ± 0.02	2.55 ± 0.02

Table 4
Relative density and mechanical properties of sintered ZrB_2 and ZrB_2/SiC ceramics.

Materials	Relative density (%)	Flexural strength (MPa)	Fracture toughness (MPa $m^{1/2}$)	Vickers hardness (GPa)	Elastic modulus (GPa)
Z	97.2 ± 0.8	546.0 ± 88.3	2.4 ± 0.1	15.4 ± 0.3	412.8 ± 44.2
ZS10	84.9 ± 2.9	427.4 ± 29.1	–	8.5 ± 1.4	343.1 ± 36.4
ZS20	99.2 ± 1.1	791.9 ± 169.6	4.0 ± 0.3	19.1 ± 0.4	471.6 ± 34.4
ZS30	99.6 ± 0.7	526.9 ± 24.8	3.0 ± 0.2	19.5 ± 0.6	525.0 ± 50.1

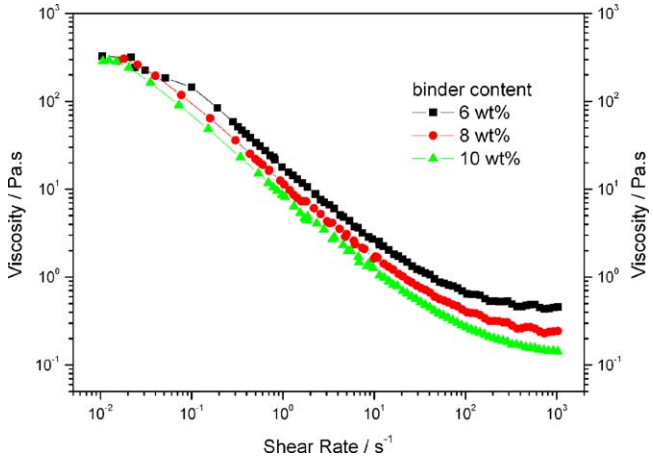

Fig. 5. Rheological properties of ZS20 suspensions with different binder content.

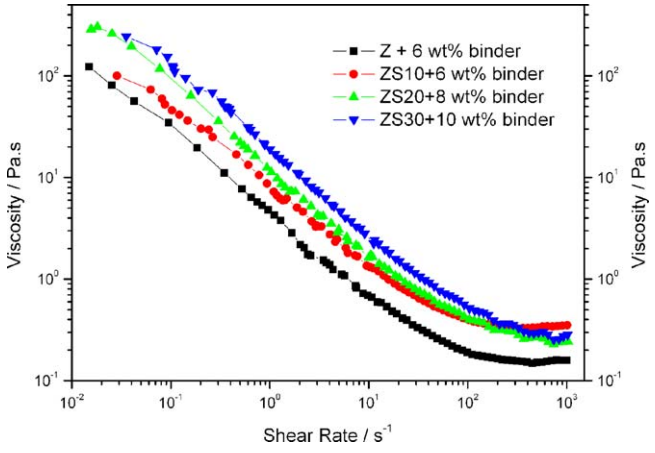

Fig. 6. Rheological properties of ZS tape casting suspensions.

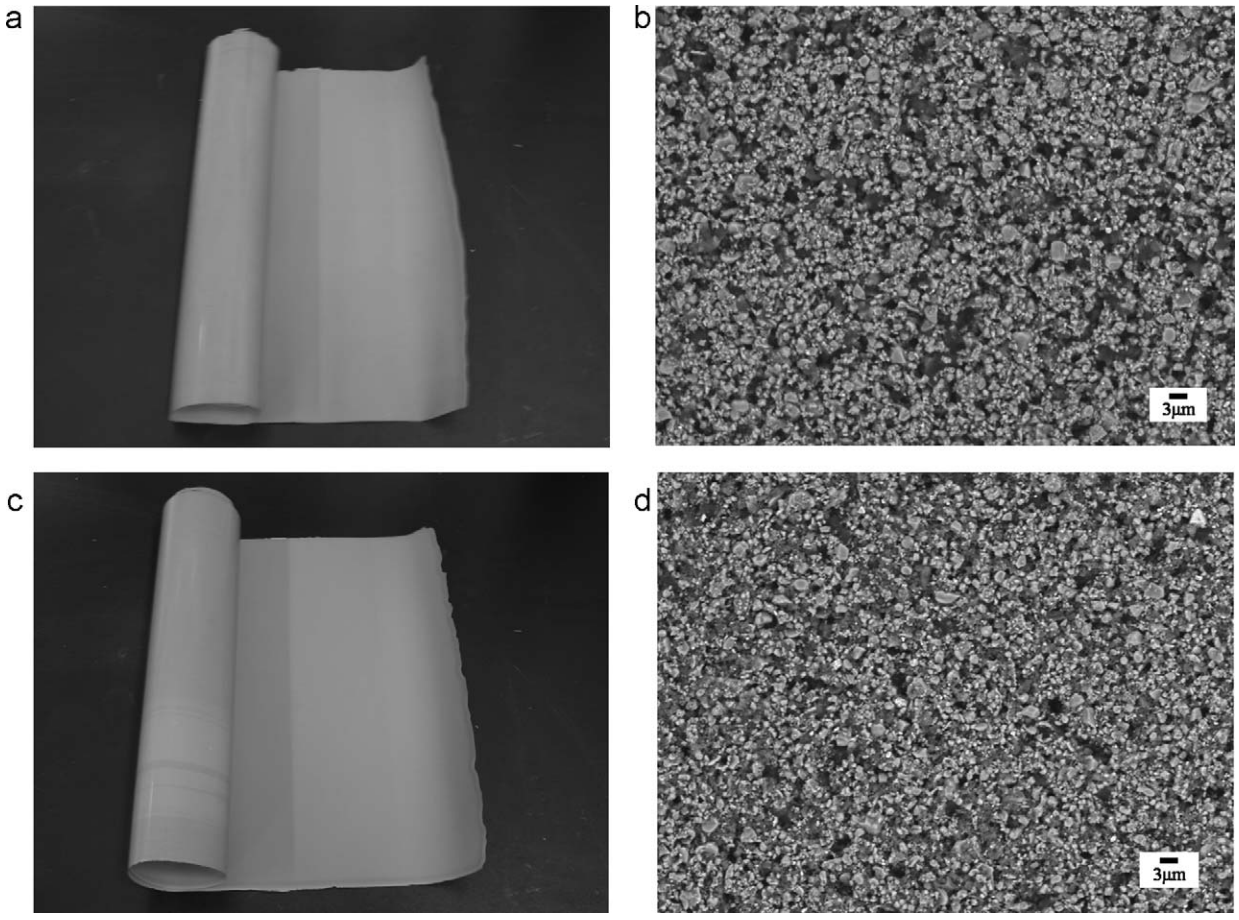

Fig. 7. ZrB_2 Green tapes: (a) overview; (b) microstructure of the surface. ZS20 Green tapes: (c) overview; (d) microstructure of the surface.

ZrB_2. Thus, 6 wt% binder was not enough to produce crack-free ZS20 green tapes. The crack-free ZS20 green tape can be obtained with 8 wt% binder content, and the green density and tensile strength were 2.65 g cm^{-3} and 1.54 MPa, respectively.

Subsequently, ZS green tapes containing different SiC content (0–30 vol%) with corresponding minimum binder content were prepared (Table 3) and rheological properties of ZS tape casting suspensions were characterized (Fig. 6). With the increase of SiC content from 10 vol% to 30 vol%, the minimum binder content required to produce crack-free tapes increased from 6 wt% to 10 wt%. Nevertheless, the tensile strength of ZS green tapes still decreased with the increase of SiC content, which confirmed that the binder had lower binding effect for SiC than for ZrB_2. The increase of SiC content and binder content together led to the decrease of green density of ZS tapes. The suspension viscosity increased with the increase of SiC content, which had been observed and discussed before. All the suspensions displayed shear thinning behavior, which is required in tape casting process because it can prevent sedimentation of ceramic particles and preserve a homogeneous distribution of the ceramic particles and of organic components in the tape by reducing the mobility of the constituents [28].

3.5. Green tapes

The dried tapes had good flexibility for handling, cutting, punching and lamination (Fig. 7(a) and (c)). There is no obvious difference in the overview between ZrB_2 green tapes and ZS20 green tapes. The green tapes had a smooth surface and homogeneous microstructure with some open pores (Fig. 7(b) and (d)). More organic phase was observed on the microstructure of ZS20 green tapes because more binder content was added into ZS20 suspension to form crack-free tapes.

3.6. Microstructure and mechanical properties of sintered samples

The relative density and mechanical properties of the as-sintered ZrB_2 and ZrB_2/SiC ceramics were shown in Table 4. The as-sintered ZrB_2 ceramic (with 6 wt% B_4C as sintering additives) had a relative density of 97.2%, which was higher than that of ZrB_2 ceramic (95.1%) using 18 wt% Mowilith emulsion as binder. The higher green density due to the low binder content resulted in higher density after sintering. The flexural strength, fracture toughness, Vickers hardness and elastic modulus of the as-sintered ZrB_2 ceramic were

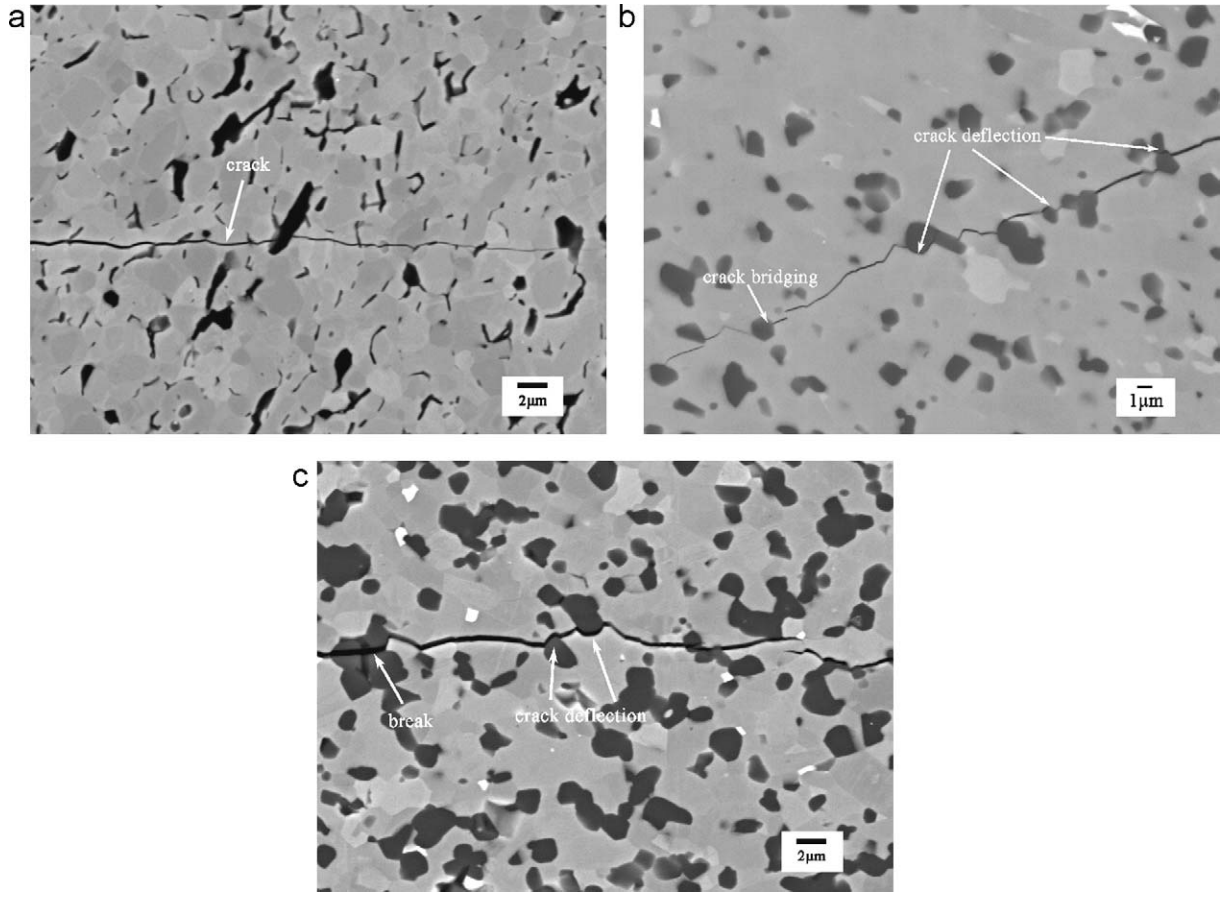

Fig. 8. Cracking propagation behaviors for (a) ZrB_2 ceramic with transgranular cracking behavior, (b) ZrB_2–20 vol% SiC ceramic with crack deflection and crack bridging behavior, and (c) ZrB_2–30 vol% SiC ceramic, showing crack deflection at small SiC particles and break of large SiC particles. In these images, ZrB_2 is gray and SiC or B_4C is black.

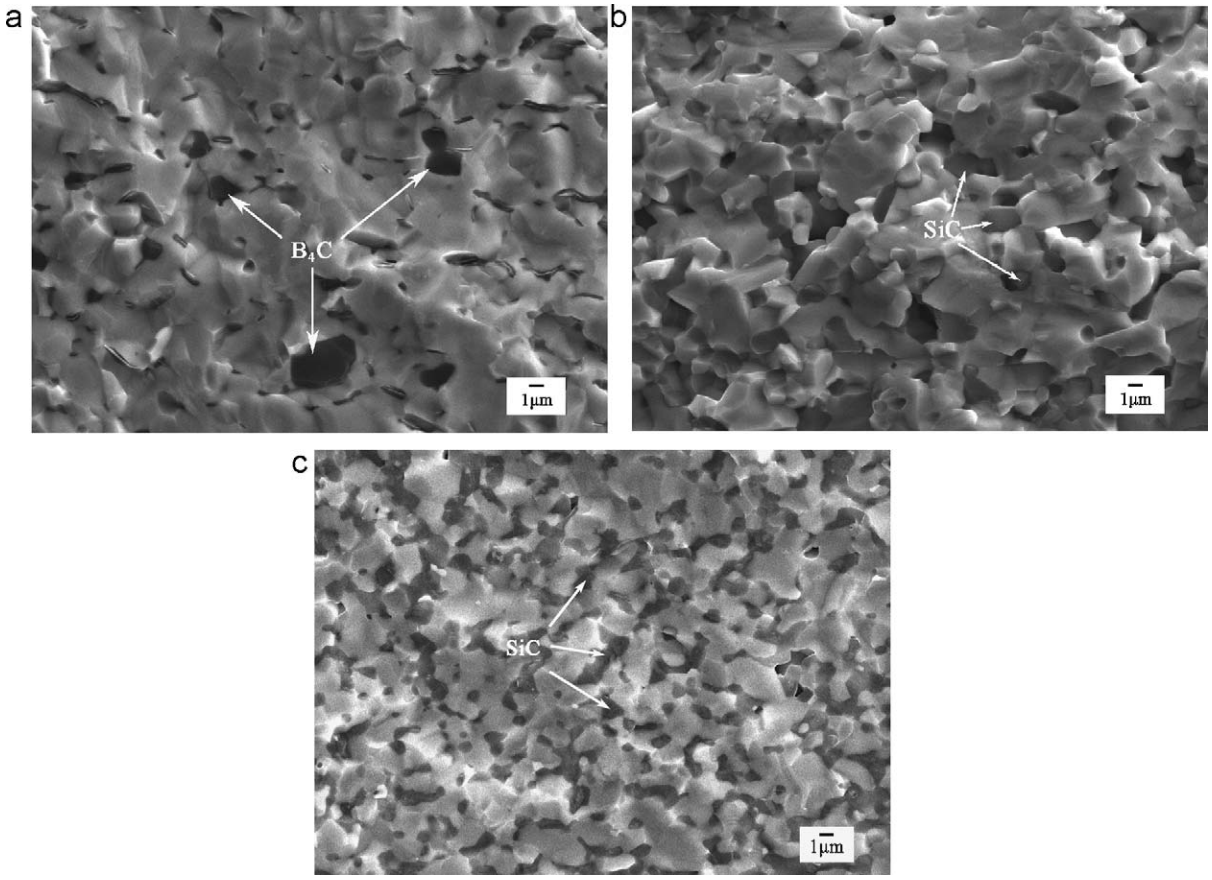

Fig. 9. SEM micrographs of fracture surface of (a) ZrB_2, (b) ZrB_2–20 vol% SiC and (c) ZrB_2–30 vol% SiC.

546.0 ± 88.3 MPa, 2.4 ± 0.1 MPa $m^{1/2}$, 15.4 ± 0.3 GPa and 412.8 ± 44.2 GPa, respectively. In combination with density measurements and SEM observation, no indication of open or closed pores was found in ZrB_2 samples containing 20 or 30 vol% SiC (relative density > 99%). However, ZrB_2 samples containing 10 vol% SiC had a rather low relative density of ~84.9%, which resulted in poor mechanical properties. In comparison, ZrB_2 samples containing 20 vol% SiC exhibited excellent mechanical properties with the flexural strength, fracture toughness, Vickers hardness and elastic modulus as 791.9 ± 169.6 MPa, 4.0 ± 0.3 MPa $m^{1/2}$, 19.1 ± 0.4 GPa and 471.6 ± 34.4 GPa, respectively.

The effect of SiC on the sinterability of ZrB_2 was that the oxidized surface layer of SiC powder could react with oxides layers on ZrB_2 powder surface and form gaseous by-products [12]. The removal of the oxides from ZrB_2 powder surface would allow the densification process occur more easily. Moreover, SiC also acted as grain-inhibitor for ZrB_2 [29]. Comparing with ZrB_2 ceramics, the higher strength of ZS20 ceramics can be attributed to the smaller ZrB_2 grain size (~1.86 μm in ZS20 ceramic and ~2.95 μm in ZrB_2 ceramic). Increased fracture toughness produced by SiC addition is probably due to the crack deflection that occurred near the SiC particles and/or at ZrB_2/SiC interfaces (Fig. 8). The crack deflection was caused by the complex residual stress state that developed during cooling from the sintering temperature due to the difference in thermal expansion coefficient between ZrB_2 and SiC.

The ZS30 ceramic showed poor flexural strength and fracture toughness compared with ZS20 samples. When SiC content further increased, the SiC particles in the matrix tended to alter from isolation to interconnected network and therefore formed larger SiC agglomerates [30]. Researches conducted by Zhu et al. [9] and Rezaie et al. [31] have demonstrated that the flexural strength of ZrB_2–SiC ceramics was controlled by the size of the SiC grains rather than the size of ZrB_2 grains. The maximum SiC grain size in ZrB_2–SiC ceramics is the strength limiting factor [9]. Here in our experiment, as shown in Fig. 8(b) and (c), the maximum SiC phase size (black phase) in ZS30 ceramics is about 9.6 μm, which is much larger than that in ZS20 ones (about 4.1 μm); that in turn resulted in sharp decrease in flexural strength. Previous report [32] has revealed that the fracture toughness of ZrB_2–SiC ceramics increased with the ratio of ZrB_2 to SiC grain size. This result was confirmed here by cracking propagation behavior test (Fig. 8). As shown in Fig. 8(b), crack deflected or bridged near SiC particles or at ZrB_2–SiC grain boundaries in ZS20 samples. While in ZS30 samples, crack only deflected around small SiC particles but went through large SiC aggregates. The crack deflections might contribute to the increase of crack length and then led to the improvement in fracture toughness. Therefore, ZS30 samples with larger SiC agglomerates showed much lower fracture toughness than ZS20 ones.

The addition of SiC to ZrB_2 ceramics resulted in an increase in hardness. This increase is attributed to two major reasons.

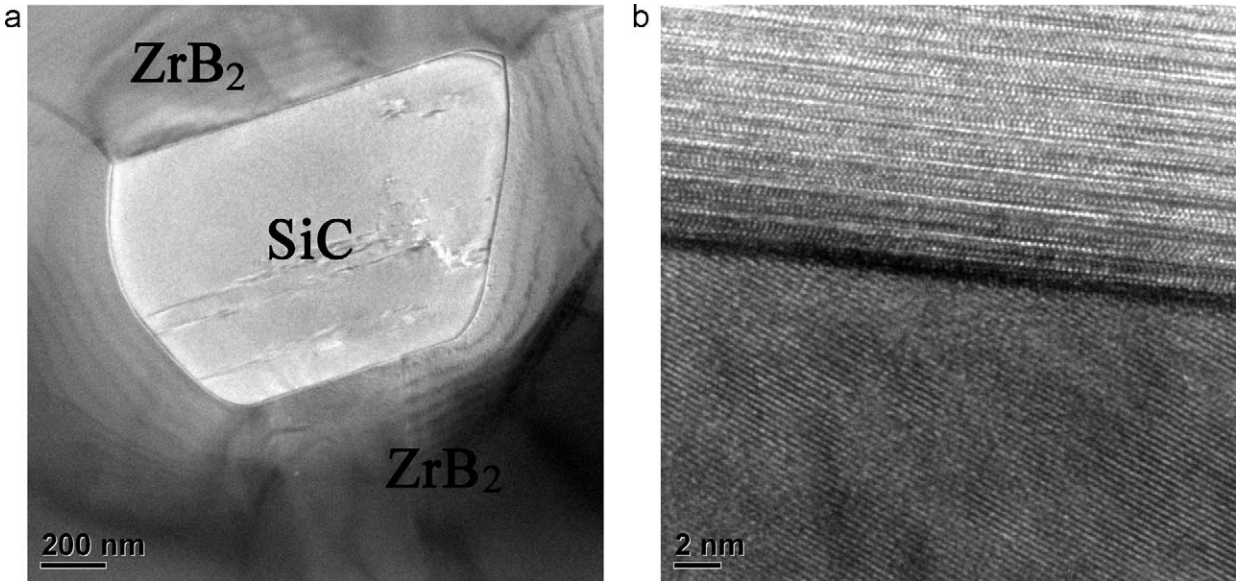

Fig. 10. TEM and HRTEM images of the sintered ZrB_2–SiC composites (a) TEM image; (b) HRTEM image.

One is the increase in density. Another is that the harness of SiC (Hv ∼ 28 GPa) is higher than that of ZrB_2 (Hv ∼ 23 GPa).

In general, the elastic modulus of pore-free ZrB_2 based composites obeys the mixture rule. However, the elastic modulus of pores-containing ZrB_2 based composites is mostly dominated by the porosity. Thus, ZS30 ceramics with highest relative density showed highest elastic modulus (525.0 GPa).

Fig. 9 displayed the SEM micrographs of the fracture surface of as-sintered ZrB_2, ZrB_2–20 vol% SiC and ZrB_2–30 vol% SiC ceramics. For ZrB_2 samples, the fracture mode was mainly intragranular fracture type and some B_4C particles were found on the fracture surface. Both intragranular and intergranular fracture mode were observed on the fracture surface of ZS20 samples. ZS30 ceramic also showed similar fracture mode as ZS20 samples. The fracture mode observed on the fracture surface was in accordance with cracking propagation behavior.

Fig. 10 showed the TEM micrographs of ZrB_2–SiC composites. As shown in Fig. 10(a), the light phase was SiC and the dark phase was ZrB_2. The SiC grains were located at triple or multiple ZrB_2 grain junctions. The samples were further observed by HRTEM (Fig. 10(b)). The ZrB_2–SiC grain boundary was clear and no amorphous or liquid phase was found. The clear grain boundary confirmed that the product of the reaction between the oxidized surface layer of SiC particles and that of ZrB_2 was not liquid phase but gaseous phase.

4. Conclusions

Stable ZrB_2–SiC suspensions with 45 vol% solid loadings were prepared in the alkaline pH range using 0.4 wt% Lopon 885 as the dispersant. The optimum binder content varied from 6 wt% to 10 wt% with the increase of SiC content from 0 vol% to 30 vol%. ZrB_2–SiC green tapes with smooth surface and homogeneous microstructure were prepared after tape casting and drying. SiC could effectively enhance the densification of ZrB_2 probably by reacting with the oxides on ZrB_2 particle surface. The as-sintered ZrB_2–20 vol% SiC ceramics had improved relative density and mechanical properties compared with ZrB_2 ceramics. The fracture surfaces of ZrB_2 and ZrB_2–SiC composites displayed a fine and uniform microstructure. The fracture mode changed from intragranular type for ZrB_2 to both intragranular and intergranular type for ZrB_2–SiC composites. The ZrB_2–SiC grain boundary was clear.

Acknowledgements

This work was supported by the National Natural Science Foundation of China (No. 50772128), the Shanghai Science and Technology Committee (No. 07DJ14001) and the State Key Laboratory of High Performance Ceramics and Superfine Microstructures.

References

[1] S.R. Levine, E.J. Opila, M.C. Halbig, J.D. Kiser, M. Singh, J.A. Salem, Evaluation of ultra high temperature ceramics for areopropulsion use, J. Eur. Ceram. Soc. 22 (14–15) (2002) 2757–2767.
[2] M.M. Opeka, I.G. Talmy, J.A. Zaykoski, Oxidation-based materials selection for 2000 °C + hypersonic aerosurfaces: theoretical considerations and historical experience, J. Mater. Sci. 39 (19) (2004) 5887–5904.
[3] D.M. Van Wie, D.G. Drewry Jr., D.E. King, C.M. Hudson, The hypersonic environment: required operating conditions and design challenges, J. Mater. Sci. 9 (19) (2004) 5915–5924.
[4] C. Morz, Zirconium diboride, Am. Ceram. Soc. Bull. 73 (6) (1994) 141–142.
[5] R.A. Culter, Engineering properties of borides, in: S.J. Schneider, Jr. (Ed.), Ceramics and Glasses, Engineered Materials Handbook, vol. 4, ASM International, Materials Park, OH, 1991, pp. 787–811.

[6] K. Upadhya, J.M. Yang, W.P. Hoffman, Materials for ultrahigh temperature structural applications, Am. Ceram. Soc. Bull. 76 (12) (1997) 51–56.
[7] F. Monteverde, A. Bellosi, Development and characterization of metal-diboride-based compositeds toughened with ultra-fine SiC particulates, Solid State Sci. 7 (2005) 622–630.
[8] Y. Yan, Z. Huang, S. Dong, D. Jiang, Pressureless sintering of high-density ZrB_2–SiC ceramic composites, J. Am. Ceram. Soc. 89 (11) (2006) 3589–3592.
[9] S. Zhu, W.G. Fahrenholtz, G.E. Hilmas, Influence of silicon carbide particle size on the microstructure and mechanical properties of zirconium diboride-silicon carbide ceramics, J. Eur. Ceram. Soc. 27 (2007) 2077–2083.
[10] S.S. Hwang, A.L. Vailiev, N.P. Padture, Improved processing and oxidation-resistance of ZrB_2 ultra-high temperature ceramics containing SiC nanodispersoids, Mater. Sci. Eng. A 464 (2007) 216–222.
[11] J. Han, P. Hu, X. Zhang, S. Meng, Oxidation behavior of zirconium diboride-silicon carbide at 1800 °C, Scripta Mater. 57 (2007) 825–828.
[12] F. Monteverde, Beneficial effects of an ultra-fine α-SiC incorporation on the sinterability and mechanical properties of ZrB_2, Appl. Phys. A 82 (2006) 329–337.
[13] D. Ni, G. Zhang, Y. Kan, Y. Sakka, Highly textured ZrB_2-based ultrahigh temperature ceramics via strong magnetic field alignment, Scripta Mater. 60 (2009) 615–618.
[14] J.A. Lewis, Colloidal processing of ceramics, J. Am. Ceram. Soc. 83 (10) (2000) 2341–2359.
[15] M. Sigmund, N.S. Bell, L. Bergström, Novel powder-processing methods for advanced ceramics, J. Am. Ceram. Soc. 83 (7) (2000) 1557–1574.
[16] A. Millán, M.I. Nieto, R. Moreno, Near-net shaping of aqueous alumina slurries using carragreenan, J. Eur. Ceram. Soc. 22 (3) (2002) 297–303.
[17] B.Q. Chen, Z.Q. Zhang, J.X. Zhang, M.J. Dong, D.L. Jiang, Aqueous gel-casting of hydroxyapatite, Mater. Sci. Eng. A 435–436 (2006) 198–203.
[18] F.F. Lange, Powder processing science and technology for increased reliability, J. Am. Ceram. Soc. 72 (1) (1989) 3–15.
[19] R.E. Mistler, Tape casting: the basic process for meeting the needs of electronics industry, Am. Ceram. Soc. Bull. 69 (6) (1990) 1022–1026.
[20] R. Moreno, The role of slip additives in tape – casting technology: part I – solvents and dispersants, Am. Ceram. Soc. Bull. 71 (10) (1992) 1521–1531.
[21] R. Moreno, The role of slip additives in tape – casting technology: part II – binders and plasticizers, Am. Ceram. Soc. Bull. 71 (11) (1992) 1647–1657.
[22] W.J. Clegg, K. Kendall, N.McN. Alford, T.W. Button, J.D. Birchall, A simple way to make tough ceramics, Nature 357 (1990) 455–457.
[23] L.J. Vandeperre, A. Kristoffersson, E. Carlström, W.J. Clegg, Thermal shock of layered ceramic structures with crack-deflecting ingerfaces, J. Am. Ceram. Soc. 84 (1) (2001) 104–110.
[24] Z.H. Lü, D.L. Jiang, J.X. Zhang, Q. Lin, Aqueous tape casting of zirconium diboride, J. Am. Ceram. Soc. 92 (10) (2009) 2212–2217.
[25] A.L. Chamberlain, W.G. Fahrenholtz, G.E. Hilmas, D.T. Ellerby, High strength zirconium diboride-based ceramics, J. Am. Ceram. Soc. 87 (6) (2004) 1170–1172.
[26] W.C.J. Wei, S.C. Wang, F.Y. Ho, Electrokinetic properties of colloidal zirconia powders in aqueous suspension, J. Am. Ceram. Soc. 82 (12) (1999) 3385–3392.
[27] B. Bitterlich, Ch. Lutz, A. Roosen, Rheology of water-based tape casting slurries, in: Proc. Euromat '99, vol. 12, Wiley-VCH, Weinheim, 2000, pp. 167–171.
[28] C. Pagnoux, T. Chartier, M.deF. Granja, F. Doreau, J.M. Ferreira, J.F. Baumard, Aqueous suspensions for tape casting based on acrylic binders, J. Eur. Ceram. Soc. 18 (1998) 241–247.
[29] R. Telle, L.S. Sigl, K. Takagi, Boride-based hard materials, in: R. Riedel (Ed.), Handbook of Ceramic Hard Materials, Wiley-VCH, Weinheim, Germany, 2000, pp. 803–945.
[30] S.C. Zhang, G.E. Hilmas, W.G. Fahrenholtz, Pressureless sintering of ZrB_2–SiC ceramics, J. Am. Ceram. Soc. 91 (1) (2008) 26–32.
[31] A. Rezaie, W.G. Fahrenholtz, G.E. Hilmas, Effect of hot pressing time and temperature on the microstructure and mechanical properties of ZrB_2–SiC, J. Mater. Sci. 42 (2007) 2735–2744.
[32] S.-Q. Guo, Densification of ZrB_2-based composites and their mechanical and physical properties: a review, J. Eur. Ceram. Soc. 29 (2009) 995–1011.